Polydispersity of a mammalian chaperone: Mass spectrometry reveals the population of oligomers in αB-crystallin

J. Andrew Aquilina*, Justin L. P. Benesch*, Orval A. Bateman†, Christine Slingsby†, and Carol V. Robinson*‡

*Department of Chemistry, Cambridge University, Lensfield Road, Cambridge CB2 1EW, United Kingdom; and †Department of Crystallography, Birkbeck College, University of London, Malet Street, London WC1E 7HX, United Kingdom

Edited by Fred W. McLafferty, Cornell University, Ithaca, NY, and approved July 24, 2003 (received for review May 16, 2003)

The quaternary structure of the polydisperse mammalian chaperone αB-crystallin, a member of the small heat-shock protein family, has been investigated by using electrospray mass spectrometry. The intact assemblies give rise to mass spectra that are complicated by the overlapping of charge states from the different constituent oligomers. Therefore, to determine which oligomers are formed by this protein, tandem mass spectrometry experiments were performed. The spectra reveal a distribution, primarily of oligomers containing 24–33 subunits, the relative populations of which were quantified, to reveal a dominant species being composed of 28 subunits. Additionally, low levels of oligomers as small as 10-mers and as large as 40-mers were observed. Interpretation of the tandem mass spectral data was confirmed by simulating and summing spectra arising from the major individual oligomers. The ability of mass spectrometry to quantify the relative populations of particular oligomeric states also revealed that, contrary to the dimeric associations observed in other small heat-shock proteins, there is no evidence for any stable substructures of bovine αB-crystallin isolated from the lens.

The small heat-shock proteins (sHSPs) constitute a family of molecular chaperones involved in protein stabilization under conditions of stress (1). The mammalian sHSP αB-crystallin is systemically expressed (2) and, along with αA-crystallin, is also a major structural protein of the eye lens. αB-crystallin has been demonstrated to display molecular chaperone activity by suppressing the aggregation of unfolded protein (3). Overexpression of αB-crystallin outside the lens is associated with a number of aberrant protein disease states including Alzheimer's, Alexander's, Parkinson's, and Creutzfeldt–Jakob diseases (4–7). Despite increasing amounts of structural information for prokaryotic (8) and plant sHSPs (9), the structures of mammalian members of this family, including the α-crystallins, HSP27 and HSP20, have yet to be elucidated. These sHSPs are isolated from tissue as polydisperse multimers, and it is this heterogeneity that has confounded the efforts of structural biologists (10, 11).

α-Crystallin, in particular, has long been the subject of conflicting results regarding its molecular mass distribution (12); however, it is accepted that from the lens, α-crystallin is isolated as a multimeric assembly ranging in molecular mass from 300 kDa to >1 MDa (10). Recently, a combination of size-exclusion chromatography and multiangle laser light scattering was used to determine the mass range of human recombinant αB-crystallin as 530–684 kDa, with a population of 585 kDa at the peak of the elution profile (13). This represents the most accurate assessment of the polydispersity inherent in the α-crystallins to date; however, it is confined to the major species in the elution profile and provides little insight into the relative populations of oligomers within the distribution.

Electrospray ionization coupled to time-of-flight mass spectrometry (MS) provides a unique insight into defining the subunit composition of noncovalent complexes (14–16) including sHSPs (17, 18) and other chaperones (19–21). It has not been possible, however, to interpret data from polydisperse proteins such as αB-crystallin. This is primarily because of their high molecular mass and the large number of oligomeric species involved, which give rise to overlapping peaks in the mass spectrum.

Tandem MS (MS/MS), a method used routinely for peptide sequencing, involves selection of ions in a well defined m/z range and subsequent collision-induced dissociation (CID) with an inert gas to produce fragment ions (22). This process can be used also to dislodge individual subunits from noncovalent assemblies of proteins (14), resulting in a redistribution of charge on the products. Here we show that by applying such an approach to αB-crystallin, we are able to define the range and the relative populations of the different oligomers that constitute this polydisperse assembly.

Materials and Methods

Purification of Bovine αB-crystallin. α-Crystallin was isolated from 2- to 4-week bovine calf lens extracts by gel filtration with a Sephacryl S300HR column (Amersham Biosciences). Protein was equilibrated into buffer A (50 mM Tris·HCl/2 mM DTT/6 M urea, pH 8.5) and concentrated to 10 mg·ml^{-1} in an ultrafiltration cell (Millipore). Samples were loaded onto a MonoQ ion-exchange column (Amersham Biosciences) and eluted with buffer B (buffer A/1 M NaCl) by using a linear gradient of 0–14% B, and peaks corresponding to the phosphorylated and unphosphorylated forms of the A and B subunits of α-crystallin were separated. The unphosphorylated αB-crystallin was concentrated to 30 mg·ml^{-1} by using a YM10 Centricon (Millipore). Seventy microliters of the sample was loaded onto a Superdex 200HR10/30 gel filtration column (Amersham Biosciences) and eluted at 0.3 ml·min^{-1} with 200 mM ammonium acetate at 4°C. Fractions of the refolded protein were collected and stored on ice to minimize quaternary structure rearrangement (23) and analyzed by MS within 1 h of collection. Equal volumes of each of the collected fractions were pooled, resulting in a combined-fractions protein concentration of 1.2 mg·ml^{-1}. An aliquot of this solution was acidified with AG 50W-X8 resin (Bio-Rad) to obtain a denatured, monomeric sample, the mass of which (20,079.2 ± 0.7 Da) agreed with the sequence mass of unphosphorylated bovine αB-crystallin of 20,078.8 Da (spectrum not shown).

MS. Experiments were conducted by using LCT (orthogonal time of flight) and modified Q-ToF 2 mass spectrometers (Micromass, Manchester, U.K.). Typically, 2 μl of solution was electrosprayed from gold-coated glass capillaries prepared in-house as described (24). To preserve noncovalent interactions on the

This paper was submitted directly (Track II) to the PNAS office.

Abbreviations: HSP, heat-shock protein; sHSP, small HSP; MS/MS, tandem MS; CID, collision-induced dissociation.

‡To whom correspondence should be addressed. E-mail: cvr24@cam.ac.uk.

LCT, the following instrument parameters were used: capillary voltage, 1.5 kV; cone gas, 150 Lh^{-1}; sample cone, 200 V; extractor cone, 10 V; ion transfer stage pressure, 9.0×10^{-3} mbar (1 mbar = 100 Pa); and ToF analyzer pressure, 3.0×10^{-6} mbar. MS/MS experiments were performed on a Q-ToF 2 instrument that had been modified for high mass operation (25). In MS mode, the following instrument parameters were used: capillary voltage, 1.6 kV; cone gas, 100 Lh^{-1}; sample cone, 200 V; extractor cone, 100 V; voltage applied to the collision cell, 4 V; ion transfer stage pressure, 9.0×10^{-3} mbar; quadrupole analyzer pressure, 9.5×10^{-4} mbar; and ToF analyzer pressure, 1.7×10^{-6} and 3.5×10^{-2} mbar of argon in the collision cell. For the MS/MS experiments, the quadrupole resolution was adjusted to encompass the entire peak of interest (30 m/z units), the extractor cone voltage was reduced to 60 V, and spectra were acquired over a range of voltages applied to the collision cell from 80 to 200 V. All spectra were calibrated externally by using a solution of cesium iodide (100 $mg \cdot ml^{-1}$) and processed with MASSLYNX software (Micromass). Spectra are shown here with minimal smoothing and without background subtraction.

Simulated Spectra. To demonstrate a theoretical deconvolution of the spectrum, individual charge-state envelopes for the different species involved were modeled. The simulated spectra shown were constructed by using SIGMAPLOT 2001 (SPSS, Chicago). Three-parameter Lorentzian curves were used to model individual peaks, with a peak width at half-height of 12 m/z units, and the intensities of the peaks were based on the observed intensities of the different charge states.

Results and Discussion

αB-crystallin eluted as a single symmetrical peak of average molecular mass ≈600 kDa when refolded from urea on a size-exclusion column (Fig. 1*A*). The corresponding spectra recorded for the fractions indicated are shown in Fig. 1*B*. The spectrum of fraction 23 (Fig. 1*B*) gave rise to a signal in the range of 8,000–15,000 m/z. Subsequent fractions, analyzed under identical MS conditions, exhibited a trend toward lower m/z values such that fraction 28 included well defined peaks within the m/z range of 6,000–12,000. At the lower m/z values, oligomeric states of αB-crystallin species in the range of 10–18 subunits, i.e., 200–361 kDa, could be identified. The unresolved portion of the spectra, as evidenced by the elevated baseline >8,000 m/z, is due to the overlap of charge series arising from a range of increasingly large oligomers of αB-crystallin.

The individual fractions were pooled to give a representative sample of all oligomers in the sample. The mass spectrum of the combined fractions gave rise to signal in the range of 7,000–15,000 m/z and lacked the clearly defined peaks at lower m/z observed for the individual later-eluting fractions (Fig. 2*A*). In fact, the smallest oligomer that could be assigned was a 16-mer, suggesting this to be the smallest oligomer present in significant amounts. The amount of information available in this spectrum is limited, because the dominant peaks do not arise from multiple charging of a single species (as in a typical electrospray spectrum) but rather from the overlap of several such series from different-sized oligomers. This is demonstrated by the intense and narrow peak at 10,040 m/z (indicated by an asterisk in Fig. 2*A*), which, because the molecular mass of a single subunit of αB-crystallin is 20,080 Da, corresponds to oligomers carrying twice as many charges as subunits.

In an attempt to identify the underlying charge-state series, MS spectra were acquired over the range of voltages applied to the collision cell from 80 to 200 V (Fig. 2*B*). In such an experiment, all ions formed during the electrospray process are indiscriminately subjected to collisions with argon atoms in the collision cell of the Q-ToF 2, resulting in the removal of excess solvent ions from the multimeric assemblies, thereby improving

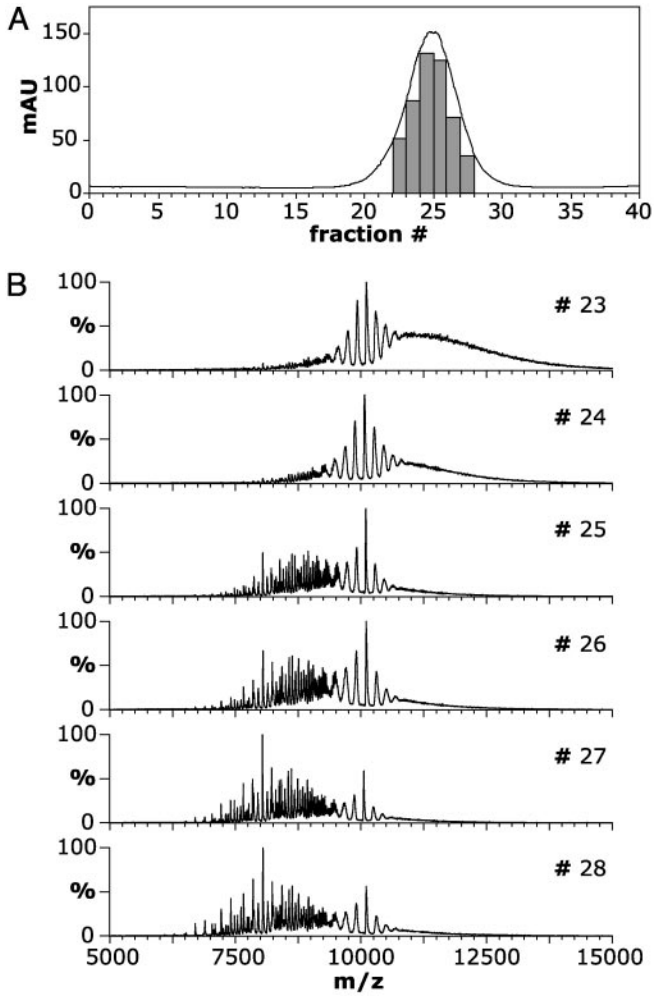

Fig. 1. Survey of the changes in mass spectra of consecutive fractions of αB-crystallin separated by size-exclusion chromatography. (*A*) Elution profile of bovine αB-crystallin refolded on column from 6 M urea into 200 mM ammonium acetate. The fractions indicated were collected and kept on ice before MS analysis. mAU, milliabsorbance units. (*B*) Electrospray mass spectra of fractions 23–28 from *A*. A shift in the distribution of ions on the m/z scale, from high to low values, was observed across the elution profile, indicating a significant decrease in the oligomeric size of αB-crystallin between fractions at the onset and tail of the peak.

the quality of the spectrum. At a voltage applied to the collision cell of 100 V, there was an increase in desolvation and consequent improvement in definition of the peaks compared with the spectrum in Fig. 2*A*. Increasing the voltage applied to the collision cell to 120 V resulted in the appearance of monomers at ≈1,500 m/z, indicating the occurrence of a CID process. It is established that noncovalent complexes subjected to CID result in the asymmetric dissociation of the oligomers into highly charged monomers and lowly charged "stripped" oligomers (18, 26–29). Because charge is conserved between dissociation products (27, 30), these stripped oligomers are observed at unusually high m/z ratios. In the spectrum obtained at 120 V, stripped oligomers can be identified >13,000 m/z, including a relatively intense peak at 20,080 m/z. The intensity of both the monomer and stripped oligomer signal increased after raising the acceleration voltage in the collision cell, and at 200 V no peaks corresponding to the original intact oligomers were observed.

The charge-state distribution of the monomers was found to shift toward higher m/z when the voltage applied to the collision

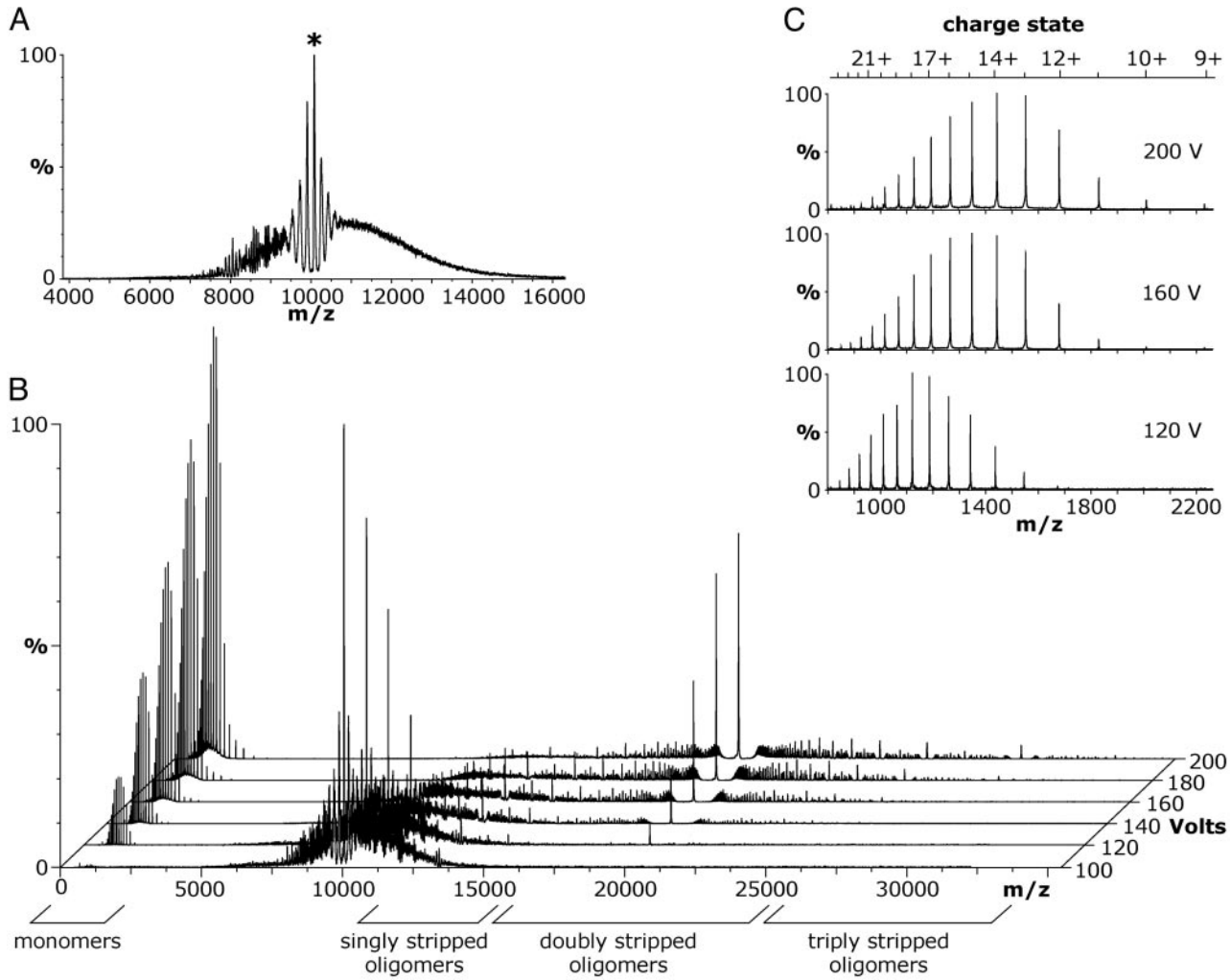

Fig. 2. (*A*) Electrospray mass spectrum of the combined fractions of bovine αB-crystallin from size-exclusion chromatography. Signal is observed between 7,000 and 15,000 m/z, with the most intense peaks at ≈10,000 m/z. These peaks are not due to a charge-state series of a single oligomer but rather to the overlap of several such series from different-sized oligomers. The spectrum was acquired at a voltage applied to the collision cell of 4 V. (*B*) Mass spectra obtained for a range of collision energies demonstrate that αB-crystallin oligomers undergo multiple loss of monomers, from one at a voltage applied to the collision cell of 120 V up to three at 200 V. (*C*) Expansion of the monomer region at voltages applied to the collision cell of 120, 160, and 200 V. The average charge state of the dissociated monomers was observed to decrease from 18+ at 120 V to 16+ at 160 V and 15+ at 200V.

cell was increased (Fig. 2*C*). The average charge state of the monomer, calculated as described (18), was found to be 18+ at 120 V, 16+ at 160 V, and 15+ at 200 V. These values were consistent with the successive loss of monomers from the oligomers, resulting in the observed stripped oligomers.[§] These observations can be summarized by the following equations:

$$n^q \rightarrow [n-1]^{q-x} + m^x$$

$$n^q \rightarrow [n-2]^{q-2y} + 2m^y$$

$$n^q \rightarrow [n-3]^{q-3z} + 3m^z,$$

where n is the number of subunits in the oligomer, q is the number of charges on the oligomer, and x, y, and z are the average charge carried by a monomer m at a given voltage applied to the collision cell. This observation of three distinct product ion series formed consecutively after increasing the voltage applied to the collision cell shows that CID of αB-crystallin results in the dissociation of an oligomer of n components into monomers and stripped oligomers of $n-1$, $n-2$, and $n-3$ subunits.

Although the definition of the peaks arising from the stripped oligomers in Fig. 2*B* was greater than for the original oligomer series, the spectra remain extremely complex and cannot be interpreted unambiguously. To obtain information about the relative populations of the various oligomers in the sample, a dissociation experiment of the polydisperse assembly was carried out by using MS/MS. This experiment involved isolation of the

[§]An αB-crystallin oligomer of ≈600 kDa (the mean molecular mass as estimated by size-exclusion chromatography in Fig. 1*A*) composed of 30 subunits would be in a 60+ charge state at 10,040 m/z. Because of the conservation of charge between dissociation products, the loss of an 18+ monomer from a $[30\text{-mer}]^{60+}$ would result in the stripped oligomer $[29\text{-mer}]^{42+}$, which would appear at 13,865 m/z. This lies within the m/z range observed for the stripped oligomers in the spectrum obtained at 120 V. At higher voltage applied to the collision cell, however, the dominant stripped oligomers appear at much higher m/z values, which can only be accounted for by the loss of more than one monomer from the original oligomers. At 160 V, the loss of two monomers carrying an average of 16+ each from a $[30\text{-mer}]^{60+}$ would result in the doubly stripped oligomer $[28\text{-mer}]^{28+}$ at 20,080 m/z. Similarly, the peaks >27,000 m/z can be accounted for by the loss of three monomers, resulting in the formation of triply stripped oligomers. Charge stripping and/or backbone cleavage of the monomers may occur in the CID process; however, for the purposes of this study these phenomena have not affected the use of the monomer charge-state distributions to interpret the dissociation products.

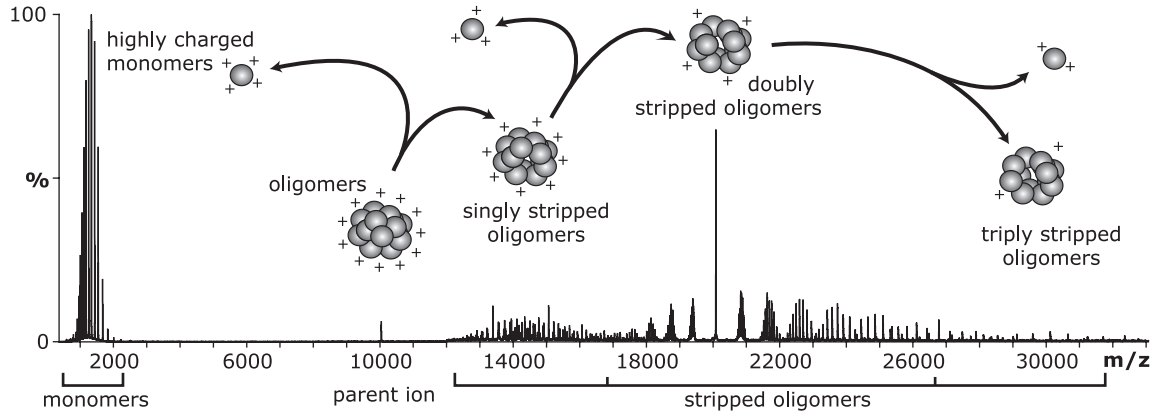

Fig. 3. MS/MS of the overlapping components in the isolated peak at 10,040 m/z (Fig. 2*A*) resulted in dissociation of the oligomers into highly charged monomers at low m/z and various stripped oligomers at high m/z values. Spectrum showing a summation of the acquisitions for a series of voltages applied to the collision cell of 80–200 V. Overlaid is a schematic showing a possible pathway for the multiple loss of monomers from a representative oligomer and the resultant mass and charge asymmetry during the gas-phase CID. The schematic shows a sequential pathway; however, we cannot rule out the simultaneous dissociation of two and three monomers from a single oligomer.

peak at 10,040 m/z (encompassing all species with two charges per subunit) and subsequent CID. A series of spectra were acquired over a range of voltages applied to the collision cell from 80 to 200 V, the combined spectrum of which is shown in Fig. 3. The precursor ion, isolated for collisional activation, is visible at 10,040 m/z. Between 12,500 and 16,500 m/z, ions arising from the removal of a single monomer from each oligomer ($n - 1$) are present. Another series of ions, attributed to the doubly stripped oligomers ($n - 2$) between 17,500 and 26,000 m/z, dominates the high m/z region of the spectrum, whereas further minor species ($n - 3$) can be seen around 30,000 m/z. A schematic illustrating the observed multiple dissociation of monomers is presented in Fig. 3.

The doubly stripped oligomer series (Fig. 3) exhibited the highest definition of peaks and the least charge-state series overlap, thereby presenting no ambiguity in interpretation. Thus, this series was used to determine the distribution of oligomeric states in the αB-crystallin assembly. Fig. 4*A* shows an expansion of the MS/MS spectrum obtained at a voltage applied to the collision cell of 130 V. At this voltage the amount of doubly stripped oligomers was at its greatest, with the amounts of singly stripped and triply stripped oligomers approximately equal. Although the spectrum remains complex, charge states corresponding to different oligomeric αB-crystallin species can readily be identified. Mass measurement allowed the unambiguous assignment of the different doubly stripped oligomers.

The dominant peak observed at 20,080 m/z corresponds to doubly stripped oligomers carrying one charge per subunit, i.e., an oligomer consisting of $n - 2$ subunits carries $n - 2$ charges. The group of peaks situated on either side of the central overlapping peak are not discreet charge-state distributions but rather are the result of contributions from the range of different-sized doubly stripped oligomers. To illustrate how this arises, a deconvolution of the experimental data in Fig. 4*A* was performed by simulating the individual charge-state distributions for the eight major doubly stripped oligomers (Fig. 4*B*). These simulations show how the dominant peak at 20,080 m/z in Fig. 4*A* arises from the overlap of peaks at this m/z from all the different doubly stripped oligomers. On either side of this m/z value the charge states do not overlap; hence, groups of peaks are observed. These simulated spectra indicate the peak series that were used to calculate the corresponding oligomer masses and demonstrate how contributions from individual components combine to give the spectrum observed for a polydisperse assembly. The ability to resolve peaks arising from the doubly stripped oligomers allowed us to quantify their relative populations. By calculating the intensities of each peak series in the region of the spectrum shown (Fig. 4*A*), we observed a symmetrical distribution of doubly stripped oligomers differing in size by one subunit, from 22 to 31 subunits, with a modal value of 26 subunits (Fig. 5). This corresponds to a distribution of oligomers in the original αB-crystallin sample of 24–33 subunits with a modal value of 28 subunits.

By its very nature, that is, isolation of a narrow m/z window, an MS/MS experiment does not take into account all the information in the MS spectrum and hence the sample. Consequently, this population distribution does not fully reflect the range of oligomers in αB-crystallin, as is evidenced by the fact that the 16-mer observed in the MS spectrum of the pooled fractions (Fig. 2*A*) was not observed in the MS/MS spectrum. Similarly, information from the high m/z region of the spectrum may have been excluded by this experiment. To investigate this, the MS (rather than MS/MS) spectrum acquired at a voltage applied to the collision cell of 200 V (Fig. 2*B*) was examined more closely. This spectrum (Fig. 6) is complicated by the fact that the groups of peaks corresponding to those observed in Fig. 4*A* contain a broader distribution of oligomers; thus they overlap, leading to ambiguity in interpretation of the entire spectrum. However, peaks additional to those in the MS/MS spectrum, which do not overlap, are observed close to the central peak at 20,080 m/z. Mass measurement using these peaks revealed that αB-crystallin was composed of minor oligomers ranging up to 40 subunits ($n - 2 = 38$) in size. Thus, when the low and high m/z regions are taken into account, the results from this study show that αB-crystallin exists as a continuum of species from 10 to 40 subunits, centered around the most highly populated assembly containing 28 subunits.

Conclusions

The use of CID in a mass spectrometer to remove up to three monomers from each αB-crystallin assembly has enabled us to define the precise oligomeric nature of this polydisperse protein, for which previously only a range of molecular masses has been reported. The advantage of using MS compared with other molecular mass determination techniques is that we are able to measure the relative populations of individual oligomeric assemblies. Moreover, we are able to define species at the extremes of the distribution, revealing oligomers as small as 10-mers and as extensive as 40-mers. This approach has the potential to determine the number of αB-crystallin subunits involved in

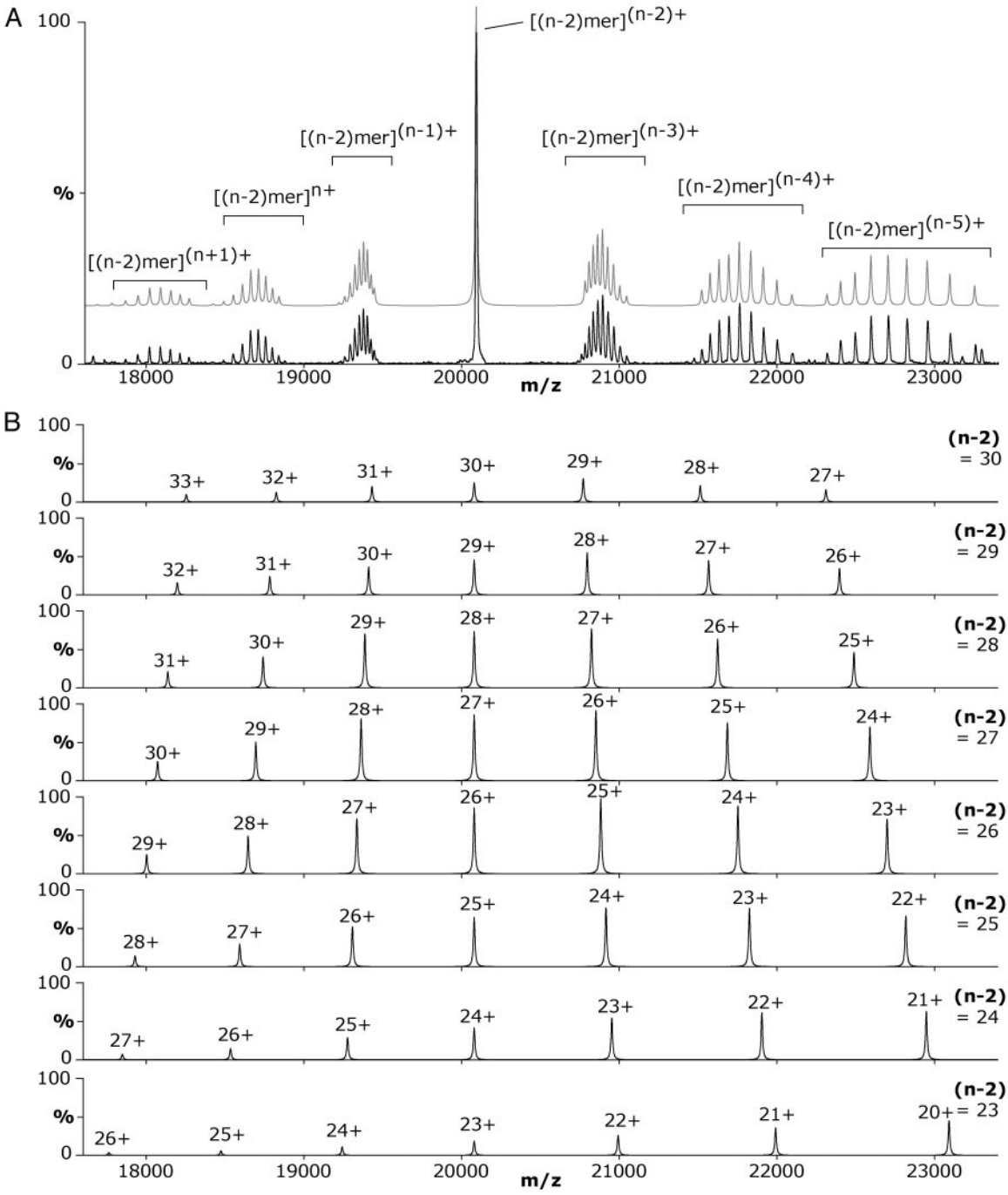

Fig. 4. (*A*) Expansion of the region of the spectrum corresponding to oligomers with $n - 2$ subunits obtained by MS/MS analysis at a voltage applied to the collision cell of 130 V. Peaks corresponding to the charge states of doubly stripped oligomers with different numbers of subunits ($n - 2$) are observed. The overlapping peak at 20,080 m/z results from oligomers carrying the same number of charges as subunits. The groups of peaks at lower m/z than this central peak result from oligomer populations carrying more than one charge per subunit ($n - 1$, n, and $n + 1$), whereas those at higher m/z arise from oligomers carrying less than one charge per subunit ($n - 3$, $n - 4$, and $n - 5$). The gray spectrum represents the sum of the simulated spectra presented in *B*. (*B*) A theoretical deconvolution of the spectrum demonstrates how several different-sized stripped oligomers combine to give the observed spectrum (*A*). Spectra for different-sized doubly stripped oligomers [$23 \leq (n - 2) \leq 30$] were simulated from the theoretical m/z values for each oligomer ion series and the observed intensities for the different charge states shown in *A*.

chaperone action and yield insights into the mechanism of substrate interaction.

sHSPs from plants, yeast, and bacteria have been shown to consist of dimeric building blocks, which have been proposed as the active unit engaged in chaperone activity, and to contribute to their monodispersity (9, 31). By contrast, the formation by αB-crystallin of oligomers containing odd and even numbers of subunits strongly implies that the monomer is the basic building block of this assembly. This intrinsic polydispersity and difference in substructure may reflect broader substrate specificity for αB-crystallin compared with the more specialized nonmammalian sHSPs. Furthermore, monomers, or variable clusters

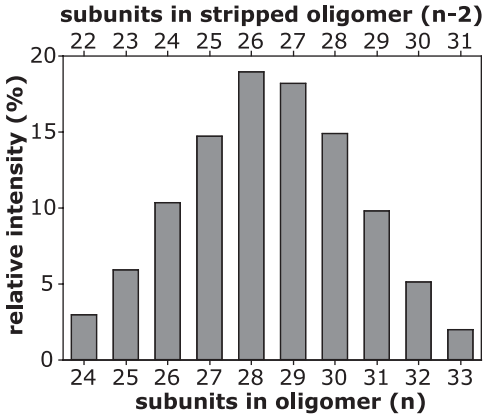

Fig. 5. Histogram showing the relative populations of the different doubly stripped oligomers ($n - 2$) formed by αB-crystallin, calculated from intensities of the peaks in the MS/MS spectrum. The population of oligomers in the original sample (n) was calculated from the doubly stripped ($n - 2$) data.

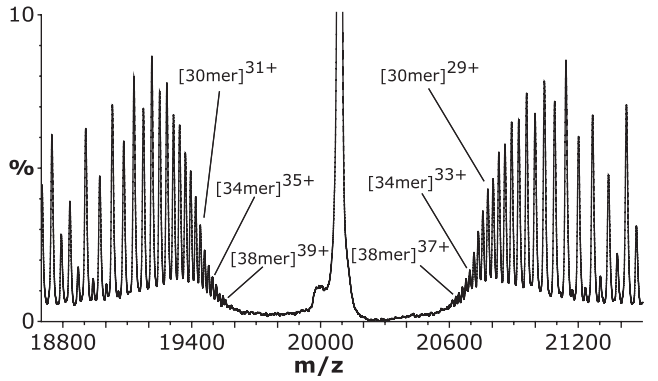

Fig. 6. Expansion of the spectrum containing the $n - 2$ oligomer series acquired at a voltage applied to the collision cell of 200 V (Fig. 2*B*) without selection of a precursor ion window. In this experiment the entire population of ions present in the sample was subjected to high-energy gas-phase collisions, giving rise to stripped oligomers for the full range of constituent assemblies. Nonoverlapping peaks proximal to the peak at 20,080 m/z provided additional information regarding the largest oligomers present in this sample.

thereof, may constitute the active units *in vivo* and contribute to an enhanced chaperone efficacy.

These results highlight the exciting possibility of defining subunit composition for other heterogeneous complexes for which only a range of molecular masses has been reported to date. Moreover, together with the ability to monitor reactions in real time (17), this technique will contribute to the understanding of the dynamics of such species and to a clearer view of their mechanism of action.

J.A.A. is a Royal Society Howard Florey Postdoctoral Fellow, J.L.P.B. is supported by the Engineering and Physical Sciences Research Council, and C.V.R. acknowledges support from the Royal Society.

1. Haslbeck, M. & Buchner, J. (2002) in *Small Stress Proteins*, eds. Arrigo, A.-P. & Muller, W. E. G. (Springer, Berlin), pp. 37–59.
2. Bhat, S. P. & Nagineni, C. N. (1989) *Biochem. Biophys. Res. Commun.* **158,** 319–325.
3. Muchowski, P. J., Bassuk, J. A., Lubsen, N. H. & Clark, J. I. (1997) *J. Biol. Chem.* **272,** 2578–2582.
4. Iwaki, T., Kume-Iwaki, A., Liem, R. K. & Goldman, J. E. (1989) *Cell* **57,** 71–78.
5. Iwaki, T., Wisniewski, T., Iwaki, A., Corbin, E., Tomokane, N., Tateishi, J. & Goldman, J. E. (1992) *Am. J. Pathol.* **140,** 345–356.
6. Renkawek, K., de Jong, W. W., Merck, K. B., Frenken, C. W., van Workum, F. P. & Bosman, G. J. (1992) *Acta Neuropathol.* **83,** 324–327.
7. Renkawek, K., Voorter, C. E., Bosman, G. J., van Workum, F. P. & de Jong, W. W. (1994) *Acta Neuropathol.* **87,** 155–160.
8. Kim, K. K., Kim, R. & Kim, S. H. (1998) *Nature* **394,** 595–599.
9. van Montfort, R. L., Basha, E., Friedrich, K. L., Slingsby, C. & Vierling, E. (2001) *Nat. Struct. Biol.* **8,** 1025–1030.
10. Haley, D. A., Horwitz, J. & Stewart, P. L. (1998) *J. Mol. Biol.* **277,** 27–35.
11. Horwitz, J. (2000) *Semin. Cell Dev. Biol.* **11,** 53–60.
12. Harding, J. J. (1997) in *Biochemistry of the Eye*, ed. Harding, J. J. (Chapman & Hall, London), pp. 94–135.
13. Horwitz, J. (2003) *Exp. Eye Res.* **76,** 145–153.
14. Sobott, F. & Robinson, C. V. (2002) *Curr. Opin. Struct. Biol.* **12,** 729–734.
15. Miranker, A. D. (2000) *Curr. Opin. Struct. Biol.* **10,** 601–606.
16. Hernández, H. & Robinson, C. V. (2001) *J. Biol. Chem.* **276,** 46685–46688.
17. Sobott, F., Benesch, J. L. P., Vierling, E. & Robinson, C. V. (2002) *J. Biol. Chem.* **277,** 38921–38929.
18. Benesch, J. L. P., Sobott, F. & Robinson, C. V. (2003) *Anal. Chem.* **75,** 2208–2214.
19. Robinson, C. V., Gross, M., Eyles, S. J., Ewbank, J. J., Mayhew, M., Hartl, F. U., Dobson, C. M. & Radford, S. E. (1994) *Nature* **372,** 646–651.
20. Bruce, J. E., Smith, V. F., Liu, C., Randall, L. L. & Smith, R. D. (1998) *Protein Sci.* **7,** 1180–1185.
21. Fändrich, M., Tito, M. A., Leroux, M. R., Rostom, A. A., Hartl, F. U., Dobson, C. M. & Robinson, C. V. (2000) *Proc. Natl. Acad. Sci. USA* **97,** 14151–14155.
22. Jennings, K. R. (2000) *Int. J. Mass Spectrom.* **200,** 479–493.
23. Bova, M. P., Ding, L. L., Horwitz, J. & Fung, B. K. (1997) *J. Biol. Chem.* **272,** 29511–29517.
24. Nettleton, E. J., Sunde, M., Lai, Z., Kelly, J. W., Dobson, C. M. & Robinson, C. V. (1998) *J. Mol. Biol.* **281,** 553–564.
25. Sobott, F., Hernández, H., McCammon, M. G., Tito, M. A. & Robinson, C. V. (2002) *Anal. Chem.* **74,** 1402–1407.
26. Light-Wahl, K. J., Schwartz, B. L. & Smith, R. D. (1994) *J. Am. Chem. Soc.* **116,** 5271–5278.
27. Schwartz, B. L., Bruce, J. E., Anderson, G. A., Hofstadler, G. A., Rockwood, A. L., Smith, R. D., Chilkoti, A. & Stayton, P. S. (1995) *J. Am. Soc. Mass Spectrom.* **6,** 459–465.
28. Versluis, C., van der Staaij, A., Stokvis, E., Heck, A. J. & de Craene, B. (2001) *J. Am. Soc. Mass Spectrom.* **12,** 329–336.
29. Felitsyn, N., Kitova, E. N. & Klassen, J. S. (2001) *Anal. Chem.* **73,** 4647–4661.
30. Jurchen, J. C. & Williams, E. R. (2003) *J. Am. Chem. Soc.* **125,** 2817–2826.
31. Narberhaus, F. (2002) *Microbiol. Mol. Biol. Rev.* **66,** 64–93.